Draft version June 20, 2018
Typeset using LaTeX **twocolumn** style in AASTeX61

ASTROPHYSICAL S-FACTORS, THERMONUCLEAR RATES, AND ELECTRON SCREENING POTENTIAL FOR THE ^{3}He(d,p)^{4}He BIG BANG REACTION VIA A HIERARCHICAL BAYESIAN MODEL

Rafael S. de Souza,[1] Christian Iliadis,[1] and Alain Coc[2]

[1] *Department of Physics & Astronomy, University of North Carolina at Chapel Hill, NC 27599-3255, USA*
[2] *Centre de Sciences Nucléaires et de Sciences de la Matière, Univ. Paris-Sud, CNRS/IN2P3, Université Paris-Saclay, Bâtiment, 104, F-91405 Orsay Campus, France*

(Received June 20, 2018)

Submitted to ApJ

ABSTRACT

We developed a hierarchical Bayesian framework to estimate S-factors and thermonuclear rates for the ^{3}He(d,p)^{4}He reaction, which impacts the primordial abundances of ^{3}He and ^{7}Li. The available data are evaluated and only those direct measurements are taken into account in our analysis for which we can estimate separate uncertainties for systematic and statistical effects. For the nuclear reaction model we adopt a single-level, two-channel approximation of R-matrix theory, suitably modified to take electron screening at low energies into account. Apart from the usual resonance parameters (resonance location and partial widths for the incoming and outgoing reaction channel), we include for the first time the channel radii and boundary condition parameters in the model evaluation. Our new analysis of the ^{3}He(d,p)^{4}He S-factor data results in improved estimates for the thermonuclear rates and associated uncertainties. This work represents the first data evaluation using R-matrix theory embedded into a hierarchical Bayesian framework, hence representing a testbed for future studies of more complex reactions.

Keywords: Bayesian

Corresponding author: Rafael S. de Souza
Corresponding author: Christian Iliadis
drsouza@ad.unc.edu,iliadis@unc.edu

1. INTRODUCTION

The big-bang theory rests on three observational pillars: primordial big-bang nucleosynthesis (BBN; Gamow 1948; Cyburt et al. 2016), the cosmic expansion (Riess et al. 1998; Peebles & Ratra 2003), and the cosmic microwave background radiation (Spergel et al. 2007; Planck Collaboration et al. 2016). The BBN takes place during the first 20 minutes after the big bang, at temperatures and densities near 1 GK and 10^{-5} g/cm^3, and is responsible for the production of the light nuclides, which play a major role in the subsequent history of cosmic evolution.

Primordial nucleosynthesis provides a sensitive test of the big bang model if the uncertainties in the predicted abundances can be reduced to the uncertainty level of the observed values. The uncertainties for the observed primordial abundances of ^{4}He, ^{2}H (or d), and ^{7}Li have been greatly reduced in recent years and amount to 1.6%, 1.6%, and 20%, respectively (Coc et al. 2015). For the observed primordial ^{3}He abundance, only an upper limit[1] is available (^{3}He/H $\leq 1.3 \times 10^{-5}$; Bania et al. 2002). At present, the uncertainties in the predicted abundances of ^{4}He, ^{2}H (or d), ^{3}He, and ^{7}Li amount to 0.08%, 2.0%, 2.8%, and 4.6%, respectively (Coc et al. 2015). The primordial abundances predicted by the big bang model are in reasonable agreement with observations, as shown in Figure 1, except for the ^{7}Li/H ratio, where the predicted value (Cyburt et al. 2016) exceeds the observed one (Sbordone et al. 2010) by a factor of $\approx$ 3. This long-standing "lithium problem" has not found a satisfactory solution yet.

Twelve nuclear processes of interest take place during big bang nucleosynthesis, (Figure 2). Among these are the weak interactions that transform neutrons into protons, and vice versa, and the p(n,γ)d reaction whose cross section can be calculated precisely using effective field theories (Savage et al. 1999). The ten remaining reactions, d(p,γ)^{3}He, d(d,n)^{3}He, d(d,p)t, t(d,n)^{4}He, t(α,γ)^{7}Li, ^{3}He(d,p)^{4}He, ^{3}He(n,p)t, ^{3}He(α,γ)^{7}Be, ^{7}Li(p,α)^{4}He, and ^{7}Be(n,p)^{7}Li, have been measured directly in the laboratory at the energies of astrophysical interest. Nevertheless, the estimation of thermonuclear reaction rates from the measured cross section (or S-factor) data remains challenging. Results obtained using traditional χ^2 minimization are plagued by a number of problems, including the treatment of systematic uncertainties and the implicit assumption

[1] Notice that the upper limit in Bania et al. 2002 is reported as "(1.1±0.2)×10^{-5}" and, unfortunately, is frequently misinterpreted as an actual mean value with an error bar.

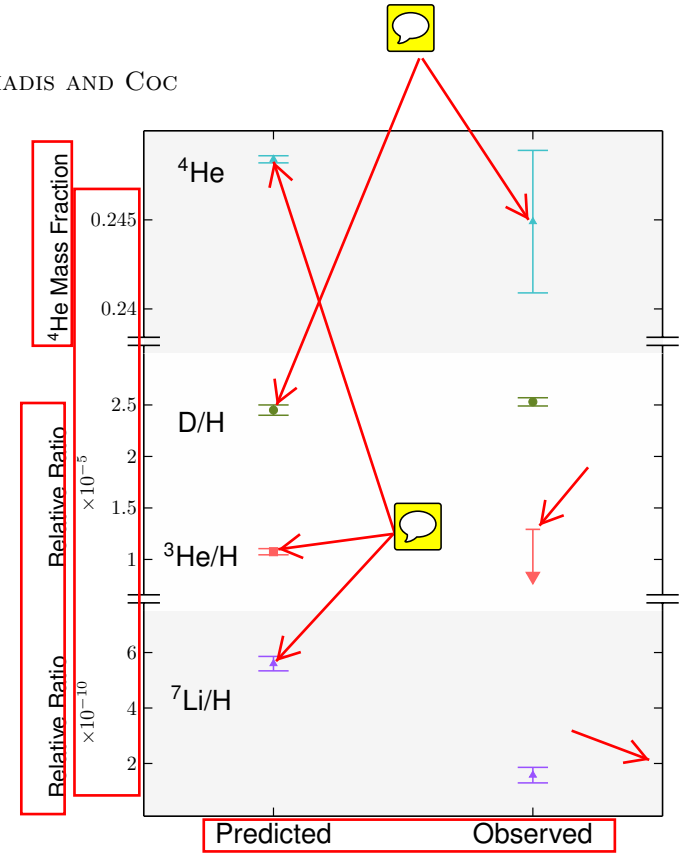

Figure 1. Predicted (left) versus observed (right) primordial abundances. For the primordial ^{3}He abundance only an upper limit is available, which we depict by a vertical arrow.

of normal likelihoods. Therefore, we have started a program to derive statistically sound big bang nucleosynthesis reaction rates using a hierarchical Bayesian model. Bayesian rates have recently been derived for d(p,γ)^{3}He, ^{3}He(α,γ)^{7}Be (Iliadis et al. 2016), d(d,n)^{3}He, and d(d,p)^{3}H (Gómez Iñesta et al. 2017). These studies adopted the cross section energy dependence from the microscopic theory of nuclear reactions, while the absolute cross section normalization was found from a fit to the data within the Bayesian framework.

We report here on Bayesian reaction rates for a fifth big bang reaction, ^{3}He(d,p)^{4}He–. This reaction marginally impacts the primordial deuterium abundance, but sensitively influences the primordial abundances of ^{3}He and ^{7}Li (Coc & Vangioni 2010). Because of its low abundance, ^{3}He has not been observed yet outside of our Galaxy. However, the next generation of large telescope facilities may allow for the determination of the ^{3}He/^{4}He ratio from observations of extragalactic metal-poor HII regions (Cooke 2015). Therefore, although a revised ^{3}He(d,p)^{4}He reaction rate is not expected to solve the ^{7}Li problem, a new rate is nevertheless desirable for improving the predicted big bang nucleosynthesis abundances.

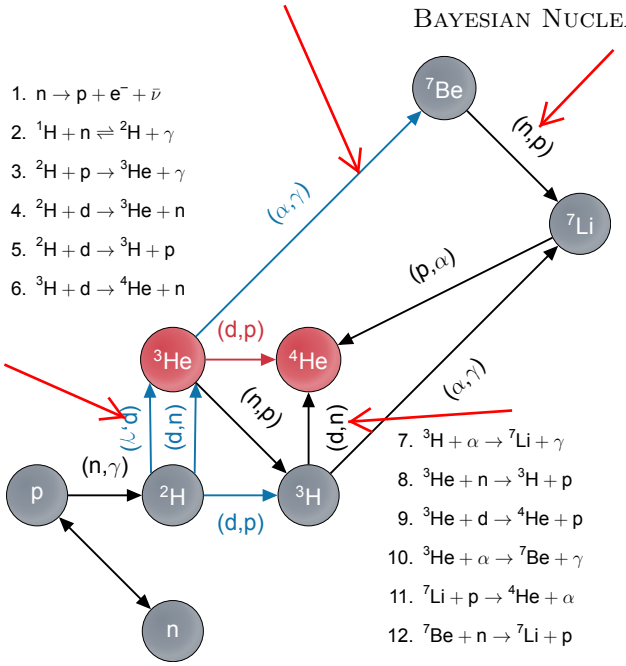

Figure 2. Nuclear reactions important for big bang nucleosynthesis. Reactions for which the rates have been obtained previously using Bayesian models are shown as blue arrows. The ^{3}He(d,p)^{4}He reaction, which is subject of the present work, is shown in red.

The ^{3}He(d,p)^{4}He reaction has been studied extensively during the past few decades, not only because of its importance to primordial nucleosynthesis, but also because it is relevant to the understanding of the electron screening effect and ~~the role of electrons in favoring deuteron-induce reactions, relevant for~~ design of future nuclear fusion reactors for energy production (e.g. La Cognata et al. 2005). At the lowest energies, the measured astrophysical S-factor shows a marked increase caused by electron screening effects. The data at those energies were used to derive the electron screening potential, but the results depended strongly on the data sets analyzed and the nuclear model applied.

In the present work, we first evaluate the available cross section data and take only those experiments into account for which we can quantify the separate contributions of statistical and systematic effects to the total uncertainty. This leaves us with seven data sets to be analyzed. For the underlying nuclear model we assume a single-level, two-channel approximation of R-matrix theory. As will be discussed below, we introduce for the first time the channel radii and boundary conditions as parameters into the statistical model. Compared to previous work (Iliadis et al. 2016; Gómez Iñesta et al. 2017), the present Bayesian study is more complicated and, therefore, represents an important testbed for future studies of even more complex systems.

In Section 2, we summarize the reaction formalism. Our Bayesian model is discussed in Section 3, including likelihoods, model parameters, and priors. In Section 4.4, we present Bayesian S-factors and thermonuclear reaction rates. A summary and conclusions are given in Section 5. Appendix A lists the data we adopted in our analysis.

2. REACTION FORMALISM

Cross section (or S-factor) data for the ^{3}He(d,p)^{4}He reaction have been fitted in the past using various assumptions, including polynomials (Krauss et al. 1987), a Padé expansion (Barbui et al. 2013), R-matrix expressions (Barker 2007), and hybrid models (Prati et al. 1994). See also Barker (2002) for a summary. Since we are mostly interested in the low-energy region where the s-wave contribution dominates the cross section, we follow Barker (1997) and describe the theoretical energy dependence of the cross section (or S-factor) using a one-level, two-channel R-matrix approximation, suitably modified to take electron screening at low energies into account.

The integrated cross section of the ^{3}He(d,p)^{4}He reaction is given by

$$\sigma_{dp}(E) = \frac{\pi}{k_d^2}\frac{2J+1}{(2j_1+1)(2j_2+1)}\,|S_{dp}|^2 \qquad (1)$$

where k_d and E are the deuteron wave number and center-of-mass energy, respectively, J = 3/2 is the resonance spin, $j_1 = 1/2$ and $j_2 = 1$ are the ground-state spins of ^{3}He and deuteron, respectively, and S_{dp} is the scattering matrix element. The corresponding bare nucleus astrophysical S-factor of the ^{3}He(d,p)^{4}He reaction, which is not affected by electron screening, is given by

$$S_{bare}(E) = Ee^{2\pi\eta}\sigma_{dp}(E), \qquad (2)$$

where η is the Sommerfeld parameter. The scattering matrix element can be expressed as (Lane & Thomas 1958)

$$|S_{dp}|^2 = \frac{\Gamma_d\Gamma_p}{(E_0+\Delta-E)^2+(\Gamma/2)^2}, \qquad (3)$$

where E_0 represents the level eigenenergy. The partial widths of the ^{3}He + d and ^{4}He + p channels (Γ_d, Γ_p), the total width (Γ), and the level shift (Δ) are given by

$$\Gamma = \sum_c \Gamma_c\ , \quad \Gamma_c = 2\gamma_c^2 P_c, \qquad (4)$$

$$\Delta = \sum_c \Delta_c\ , \quad \Delta_c = -\gamma_c^2(S_c - B_c), \qquad (5)$$

where γ_c^2 is the reduced width, and B_c is the boundary condition parameter. The energy-dependent quantities

P_c and S_c denote the penetration factor and shift factors, respectively, for channel c (either d + ^{3}He or p + ^{4}He), which are computed from the Coulomb wave functions, F_l and G_l, according to:

$$P_c = \frac{k_d a_c}{F_\ell^2 + G_\ell^2}, \qquad S_c = \frac{k_d a_c (F_\ell F'_\ell + G_\ell G'_\ell)}{F_\ell^2 + G_\ell^2}. \quad (6)$$

The Coulomb wave functions and their derivatives are evaluated at the channel radius, a_c; ℓ denotes the orbital angular momentum for a given channel.

The R-matrix channel radius is usually expressed as

$$a_c = r_0 \left(A_1^{1/3} + A_2^{1/3} \right) \quad (7)$$

where A_1 and A_2 are the mass numbers of the two interacting nuclei; r_0 denotes the radius parameter, with a value customarily chosen between 1 fm and 2 fm. For the ^{3}He(d,p)^{4}He reaction, previous choices for the channel radii ranged between 3 fm and 6 fm (e.g., Barker 2002; Descouvemont et al. 2004). R-matrix parameters and cross sections derived from data have a well-known dependence on the channel radii, which arises from the truncation of the R-matrix to a restricted number of poles (i.e., a finite set of eigenenergies). The radius of a given channel has no rigorous physical meaning, except that the chosen values should exceed the sum of the radii of the colliding nuclei (e.g. Descouvemont & Baye 2010). We will discuss the impact of varying the channel radii on our derived S-factors in Section 4.

For a narrow resonance, the observed resonance energy, E_r, i.e., the peak of the observed cross section or S-factor, can be defined as:

$$E_0 + \Delta(E_r) - E_r = 0. \quad (8)$$

The boundary condition parameter is then chosen as:

$$B_c = S_c(E_r), \quad (9)$$

so that the level shift becomes zero at the observed resonance energy ($E_r = E_0$). This assumption, corresponding to setting the eigenenergy (E_0) equal to the observed resonance energy (E_r) in the data fitting, has been adopted in most previous studies (e.g., Barker 2007). However, it does not necessarily apply to broad resonances, where the maximum of the scattering matrix element, cross section, and S-factor peak at different energies. Indeed, for the low-energy ^{3}He(d,p)^{4}He resonance, the total observed width is approximately equal to the observed resonance energy. We will investigate in Section 4 the impact of varying the boundary condition parameters on our results.

In laboratory experiments, electrons are usually bound to the interacting projectile and target nuclei.

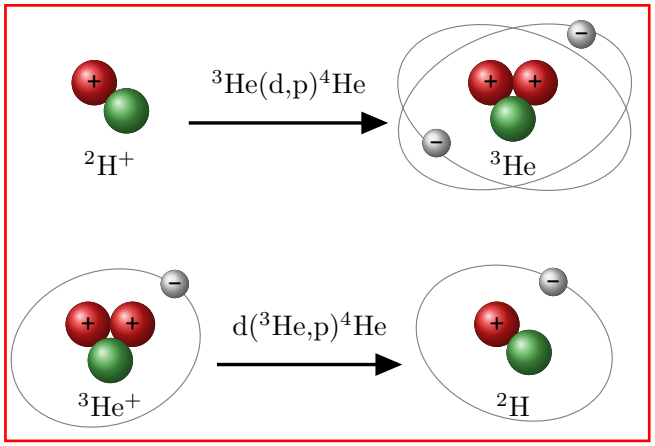

Figure 3. Illustration of the different processes involved in the ^{3}He(d,p)^{4}He and d(^{3}He,p)^{4}He reactions. (Top) Deuterium ion beam (with no atomic electron) incident on a neutral ^{3}He target atom (two atomic electrons). (Bottom) ^{3}He ion (with one atomic electron) incident on a neutral deuterium target atom (one atomic electron). The electron screening effect is of different magnitude in these two situations.

These electron clouds effectively reduce the Coulomb barrier of the interaction nuclei and give rise to an increasing transmission probability. We perform the S-factor fit to the data using the expression (Assenbaum et al. 1987; Engstler et al. 1988):

$$S(E) \approx S_{bare}(E) e^{\pi\eta(U_e/E)}, \quad (10)$$

where U_e is the energy-independent electron screening potential.

Notice that the measurement can be performed in two ways, depending on the identity of the projectile and target. The situation is shown in Figure 3. The notation ^{3}He(d,p)^{4}He refers to a deuterium ion beam (without atomic electrons) directed onto a neutral ^{3}He target (two electrons), while d(^{3}He,p)^{4}He refers to a ^{3}He ion beam (one electron) directed onto a neutral deuterium target (one electron). These two situations result in different electron screening potentials, U_e. The distinction is particularly important at center-of-mass energies below 50-keV, as will be shown below.

3. BAYESIAN MODEL

3.1. *General aspects*

Bayesian probability theory provides a mathematical framework to infer, from the measured data, the degree of plausibility of model parameters. (Jaynes & Bretthorst 2003). It allows to update a current state of knowledge about a set of model parameters, θ, in view of newly available information. The updated state of knowledge about θ is described by the posterior distributions, $p(\theta|y)$, i.e., the probability of the parameters,

θ, given the data, y. At the foundation of the theory lies ~~the~~ Bayes' theorem:

$$p(\theta|y) = \frac{\mathcal{L}(y|\theta)\pi(\theta)}{\int \mathcal{L}(y|\theta)\pi(\theta)d\theta}. \quad (11)$$

The ~~right term~~ of Equation 11 represents the product of the model likelihood, $\mathcal{L}(y|\theta)$, i.e., the probability that the data, y, were obtained given the model parameters, θ, and the prior distribution, $\pi(\theta)$, which represents our state of knowledge before considering the new data. The normalization factor appearing in the denominator, called the evidence, describes the probability of obtaining the data considering all possible parameter values.

In the Bayesian framework, the concept of hierarchical Bayesian models is of particular interest when accounting for different effects and processes that impact the measured data (Parent & Rivot 2012; de Souza et al. 2015, 2016; Hilbe et al. 2017). The underlying idea is to decompose higher-dimensional problems into a number of probabilistically linked lower-dimensional substructures. Hierarchical Bayesian models ~~enable us to include in a coherent fashion~~ ~~the~~ different types of uncertainties into the model, thereby solving inferential problems that are not amenable to traditional statistics (Trotta 2017).

3.2. *An example*

Figure 4 depicts a simple example for a nuclear counting experiment to illustrate an inherently hierarchical statistical structure. The vertical axis shows the number of counts and the different layers of variabilities are indicated on the horizontal axis. The theoretical mean value of the ~~number of counts~~, y (grey dot), is unknown. In statistical parlance, y is called a latent or hidden variable, representing the boundary between the theoretical and observable world. The actual number of decays, y' (blue dot), differs from the theoretical mean value because of the stochastic nature of a nuclear decay or reaction ~~processes~~. We can write

$$y' = y + \epsilon_{stoc}, \quad (12)$$

where ϵ_{stoc} quantifies the stochastic contribution that perturbs y. The quantity y' is also unobservable since we have not considered experimental effects yet. Typically, data are subject to systematic and statistical effects.

The systematic contribution, ϵ_{syst}, which affects all data points of a given experiment equally, perturbs the number of counts (blue dot) and gives rise to the green dot. We can write

$$y'' = y' + \epsilon_{syst}, \quad (13)$$

Finally, the statistical contribution, ϵ_{stat}, which differs for each data point of a given experiment, also perturbs

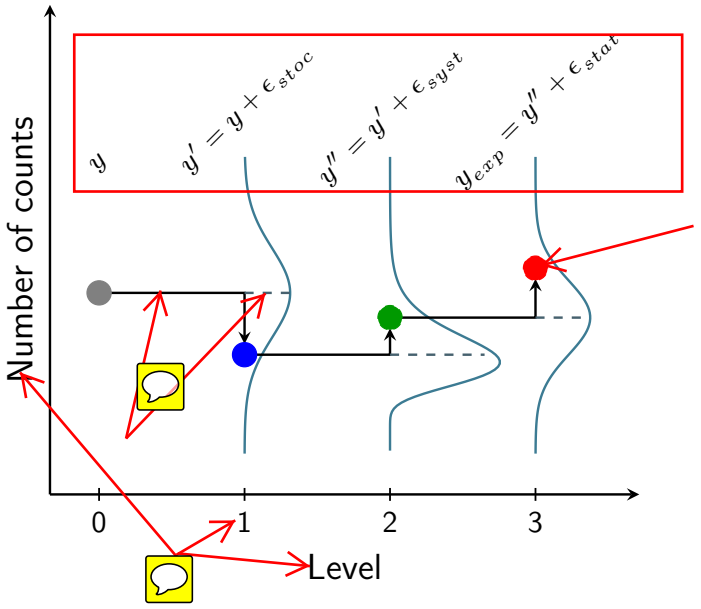

Figure 4. Example of a counting experiment. The true (but unknown) value of the quantity, y (here the mean number of ~~counts~~; gray circle) is perturbed at each level by different effects: (i) intrinsic stochasticity (ϵ_{stoc}; blue circle), (ii) experimental systematic effects (ϵ_{syst}; green circle), (iii) experimental statistical effects (ϵ_{stat}; red circle). The Bayesian model is constructed to estimate the posterior density for the true value of y (gray circle) from the actual measurement (red circle). The probability densities at each level are shown as solid blue lines.

the number of counts (green dot) and gives rise to the measured value (red dot), according to

$$y_{exp} = y'' + \epsilon_{stat}. \quad (14)$$

It is straightforward to construct the hierarchical Bayesian model that incorporates all of these different layers of variability, as explained in the next section. The goal is to estimate the posterior density for the unobservable theoretical mean, y, based on the measured value of y_{exp}.

3.3. *Likelihoods and priors*

We will next discuss how to construct likelihoods to quantify the different layers of uncertainty affecting the ^{3}He(d,p)^{4}He and d(^{3}He,p)^{4}He data. Throughout this work, we evaluate the Bayesian models using JAGS ("Just Another Gibbs Sampler"), a program for analysis of Bayesian hierarchical models using a Markov chain Monte Carlo framework (Plummer 2003). Specifically, we used the RJAGS package to interface JAGS with the R language (Team 2010).

Running a Bayesian model in JAGS refers to generating random samples from the posterior distribution of model parameters. This requires the definition of

the model, likelihoods, and priors, as well as the initialization, adaptation, and monitoring of the Markov chain. We implemented a new JAGS module to allow for sampling of a theoretical S-factor model for the ^{3}He(d,p)^{4}He reaction based on the R-matrix formalism (Section 2), including the effect of electron screening.

3.3.1. *Stochastic effects*

We will first discuss the treatment of a stochastic process. Suppose an experimental S-factor, S_{exp}, is free of systematic and statistical measurement uncertainties ($\epsilon_{syst} = 0$, and $\epsilon_{stat} = 0$), but is subject to an unknown stochastic effect ($\epsilon_{stoc} \neq 0$). If the variable under study is continuous, one can assume in the simplest case a Gaussian noise, with standard deviation of σ_{stoc}. The model likelihood connecting experiment with theory, assuming a vector of model parameters, θ, is then given by:

$$\mathcal{L}(S_{exp}|\theta) = \prod_{i=1}^{N} \frac{1}{\sqrt{2\pi\sigma_{stoc}^2}} \exp\left[-\frac{(S_{exp;i} - S_i(\theta))^2}{2\sigma_{stoc}^2}\right], \tag{15}$$

where $S_i(\theta)$ is the model S-factor (obtained from R-matrix theory), and the product runs over all data points, N, labeled by i. In symbolic notation, this expression can be written as:

$$S_{exp;i} \sim \text{Normal}(S_i(\theta), \sigma_{stoc}^2) \tag{16}$$

implying that the experimental S-factor datum, i, is sampled from a normal distribution, with a mean equal to the true value, $S_i(\theta)$, and a variance of σ_{stoc}^2.

3.3.2. *Statistical effects*

Any experiment is subject to measurement uncertainties, which are the consequence of an inherent imperfection of the data taking process. Suppose the measurement uncertainties are solely given by statistical effects and that the likelihood can be described, in the simplest case, by a normal probability density. The likelihood for such model can be written symbolically as:

$$S_{exp;i} \sim \text{Normal}(S_i(\theta), \sigma_{stat;i}^2). \tag{17}$$

where $\sigma_{stat;i}^2$ represents the variance of the normal density for datum i. Unlike the uncertainty caused by the effect of stochasticity (Section 3.3.1), statistical uncertainties can be reduced by improving the data collection procedure and by collecting more data.

When both statistical and stochastic uncertainties are present, the model can be easily extended to accommodate both effects. The likelihood for such model is given by the nested expressions:

$$S_i' \sim \text{Normal}(S_i(\theta), \sigma_{stoc}^2) \tag{18}$$

$$S_{exp;i} \sim \text{Normal}(S_i', \sigma_{stat;i}^2) \tag{19}$$

These expressions provide an intuitive view of how a chain of probabilistic disturbances can be combined into a hierarchical structure. First, stochastic effects, quantified by the standard deviation σ_{stoc} of a normal probability density, perturb the theoretical value of a given S-factor datum, $S_i(\theta)$, to produce a value of S_i'; second, the latter value is in turn perturbed by the statistical uncertainty, quantified by standard deviation $\sigma_{stat;i}$ of a normal probability density, to produce the measured value $S_{exp;i}$. The above demonstrates how any effect impacting the data can be implemented in a straightforward manner into a Bayesian data analysis.

3.3.3. *Systematic effects*

Systematic uncertainties are usually not reduced by combining the results from different measurements or by collecting more data. Reported systematic uncertainties are based on assumptions made by the experimenter, are model-dependent, and follow vaguely known probability distributions (Heinrich & Lyons 2007). In a nuclear counting experiment, systematic effects impact the overall normalization by shifting all points of a given data set into the same direction, and they are often quantified by a multiplicative factor.

For example, if the systematic uncertainty for a given data set is reported as $\pm 10\%$ (i.e., $\sigma_{syst} = 0.10$), the factor uncertainty amounts to 1.10. A useful distribution for normalization factors is the lognormal probability density:

$$f(x) = \frac{1}{\sigma_L x\sqrt{2\pi}} \exp\left[-\frac{(\ln x - \mu_L)^2}{2\sigma_L^2}\right], \tag{20}$$

which is characterized by two quantities, the location parameter, μ_L, and the shape parameter, σ_L. The median value of the lognormal distribution is given by e^{μ_L}, while the factor uncertainty, for a coverage probability of 68%, is e^{σ_L}. In our model, we include a systematic effect as an informative lognormal prior with a median of 1.0, i.e., $\mu_L = 0$, and a factor uncertainty given by the systematic uncertainty, i.e., in the above example, $\sigma_L = \ln(1.10)$. In our above model, we can include systematic uncertainties using the nested expressions:

$$S_i' \sim \text{Normal}(S_i(\theta), \sigma_{stoc}^2) \tag{21}$$

$$S_{exp;i,j} \sim \text{Normal}(\xi_j S_i', \sigma_{stat;i}^2), \tag{22}$$

where ξ_j denotes the normalization factor for data set j.

3.3.4. *Priors*

To test the effects of different priors on our results, we consider two scenarios. In the first scenario ("case I"),

Table 1. Priors choices for Case I (moderately informative) and II (weakly informative)[a].

	Case I	Case II
E_0	HalfNormal(0,1)	HalfNormal(0, 1)
E_r	E_0	HalfNormal(0, 1)
γ_d^2	HalfNormal(0,1)	HalfNormal(0,1)
γ_p^2	HalfNormal(0,1)	HalfNormal(0,1)
a_d	6	HalfNormal(6,1)
a_p	5	HalfNormal(5,1)
U_e	HalfNormal(0, 0.1^2)	HalfNormal(0, 0.1^2)
ξ	LogNormal(0, σ_L^2)[b]	LogNormal(0, σ_L^2)[b]

[a] Units for energies are in MeV, while those for the channel radii are in fm.
[b] $\sigma_L \equiv \ln(1+\sigma_{syst}^2)$.

we employ moderately informative priors for the eigenvalue (E_0) and reduced widths (γ_d^2, γ_p^2), and fixed values for the channel radii ($a_d = 6$ fm, $a_p = 5$ fm), consistent with Barker (2007). We will also set the eigenvalue, E_0, equal to the observed resonance energy, E_r, in the data fitting. In the second scenario ("case II"), we adopt weakly informative priors for E_0, E_r, γ_d^2, γ_p^2, a_d, and a_p.

As for the electron screening potential, Aliotta et al. (2001) obtained values of $U_e = 146 \pm 5$ eV for the d(^{3}He,p)^{4}He reaction, and $U_e = 201 \pm 10$ eV for the ^{3}He(d,p)^{4}He reaction. Since U_e is a positive quantity, we will adopt a weakly informative prior given by a half-normal distribution (i.e., a normal distribution left-truncated at zero) with a standard deviation of 100 keV.

As already pointed out above, lognormal priors are adopted for the normalization factors, ξ_j, of each experiment, j. They are given by:

$$\xi_j \sim \text{LogNormal}(0, \ln(1+\sigma_{syst;j}^2)), \tag{23}$$

where $\sigma_{syst;j}$ denotes the systematic uncertainty for data set j. Table 1 summarizes our choices of priors for the two scenarios.

4. ANALYSIS OF ^{3}He(d,p)^{4}He AND DATA

The current status of the available data for the ^{3}He(d,p)^{4}He and d(^{3}He,p)^{4}He reactions is discussed in detail in Appendix A. For the present analysis, we adopt the results of Zhichang et al. (1977); Krauss et al. (1987); Möller & Besenbacher (1980); Geist et al. (1999); Costantini et al. (2000); Aliotta et al. (2001), because only these data sets allow for a separate estimation of statistical and systematic uncertainties. In total, our analysis includes 214 data points at center-of-mass energies between 4.2 keV and 471 keV.

4.1. *Case I*

The hierarchical Bayesian model, using case I as an example, can be summarized as:

Likelihoods

$$S_i' \sim \text{Normal}(S_i(\theta)e^{\pi\eta(U_{e;k}/E_{exp;i})}, \sigma_{stoc}^2)$$
$$S_{exp;i,j} \sim \text{Normal}(\xi_j S_i', \sigma_{stat;i}^2) \tag{24}$$

Parameters

$$\theta \equiv (E_r, \gamma_d^2, \gamma_p^2, U_{e;k}, \xi_j)$$

Priors

$$\xi_j \sim \text{LogNormal}(0, \ln(1+\sigma_{\text{syst;j}}^2))$$
$$(E_0 \equiv E_r, \gamma_d^2, \gamma_p^2) \sim \text{HalfNormal}(0,1)$$
$$U_{e;k} \sim \text{HalfNormal}(0, 0.01)$$

Indices

$$j = 1, ..., 7; \quad k = 1 \text{ or } 2; \quad \text{i} = 1, ..., 214$$

The first layer accounts for the effects of an inherent stochastic uncertainty and electron screening, while the second layer describes the effects of systematic and statistical uncertainties. The indices denote the number of data sets (j), data points (i), and the two possibilities for electron screening depending on the kinematics of the experiment (k).

The MCMC sampling will provide the posteriors for all 12 parameters. We generated random samples using three independent Markov chains, each of length 20,000 (without burn-in). This ensures that the Monte Carlo fluctuations are negligible compared to the statistical and systematic uncertainties. The lengths of the initial adapting and burn-in phases were set to 5,000 steps. The fitted model is displayed at figure 5. The plot shows three solutions and their respective credible intervals: The bare S-factor (purple intervals), i.e. the estimated S-factor free from the effects of electron screening, and the solution for d(^{3}He,p)^{4}He (red intervals) and ^{3}He(d,p)^{4}He (gray intervals) datasets. The inset highlights the region which the effects of electron screening starts to be non-negligible.

For Case I, the one- and two-dimensional marginalized posterior densities of the R-matrix parameters E_0, γ_d, γ_p, U_e are shown in Figure 6, in addition we included the posteriors for the estimated S-factor at zero energy. The contours in the panels for the two-dimensional densities depict 68%, 95%, and 99.7% credible intervals around the marginal posterior mean.

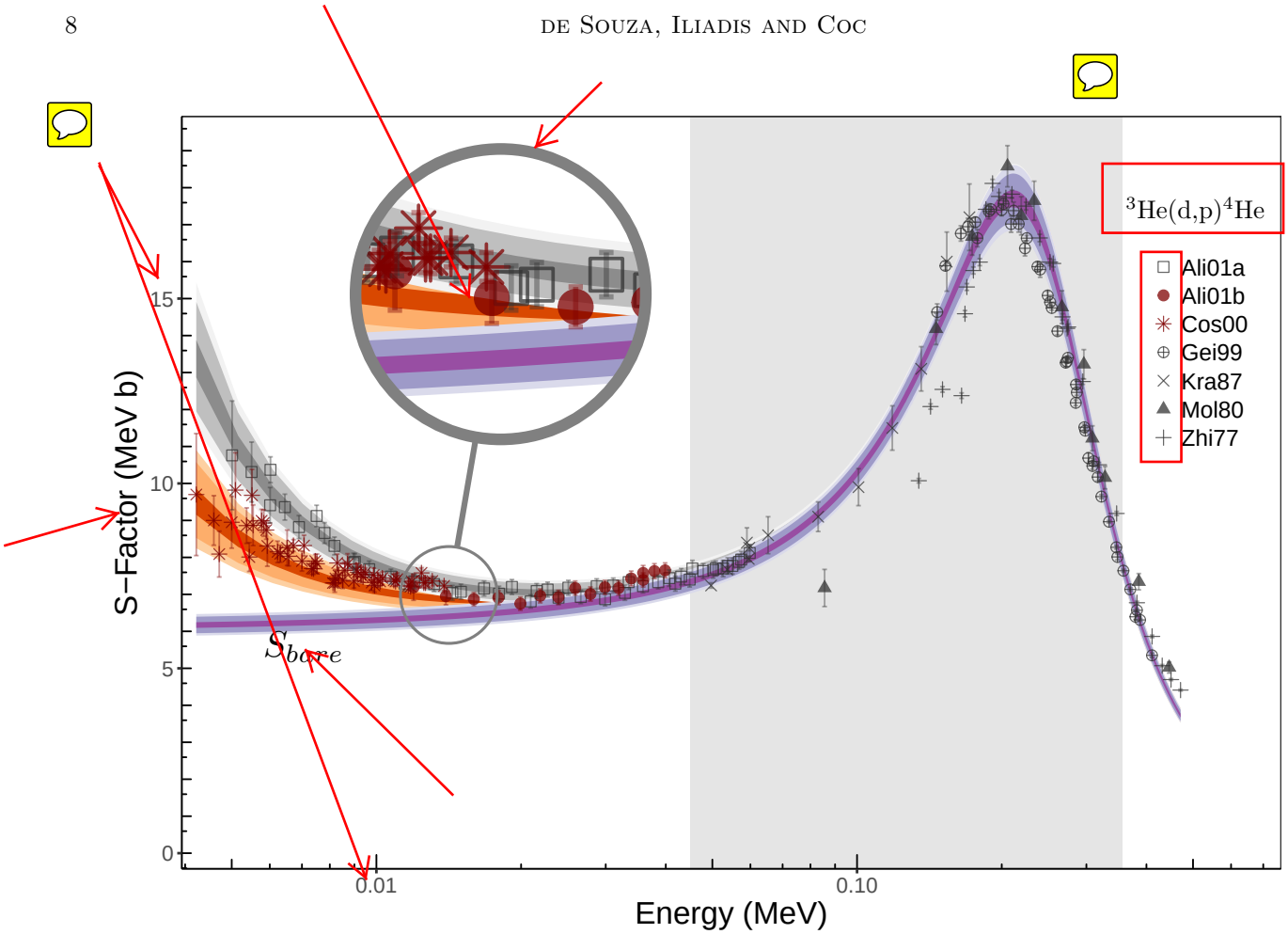

Figure 5. ~~Bayesian~~ Astrophysical S-factor ~~for the~~ bare and screened nuclei versus ~~^{3}He + d~~ center-of-mass energy ~~for the ^{3}He(d,p)^{4}He reaction~~. The symbols ~~show the data of each independent generated group~~. ~~The error~~ bars refer to (~~1~~) statistical uncertainties only. The shaded areas depicts 50%, 95% , and 99% credible intervals around the mean S-~~factor~~.

4.2. *Case II*

The hierarchical Bayesian model for case II, can be easily extended from the model 24 by replacing the priors on E_r, a_d, and a_p following 1. The one- and two-dimensional marginalized posterior densities for its R-matrix parameters in addition to the estimated S-factor at zero energy. are shown in Figure 7. The contours in the panels for the two-dimensional densities depict 68%, 95%, and 99.7% credible intervals around the marginal posterior mean.

The inclusion of the channels radii a_d, and a_p as additional free parameters induces highly degeneracy and multi-modality in the posteriors. The weakly constrained capability have been previously identified in e.g. Descouvemont & Baye (2010). The screening-potential and the S-factor at zero energy are marginally affected by the prior choices or assumed values of the channel radii. In what follows, we compare our estimated parameters with previous estimates and their subsequent impact in the thermonuclear reaction rates.

4.3. *Previous results*

Previous estimates based on χ^2 optimization have been applied to the calculation of ^{3}He(d,p)^{4}He R-matrix parameters (Barker 2007), screening effects (Descouvemont et al. 2004) and reaction rates Descouvemont et al. (2004); Xu et al. (2013).

A summary statistics of our analysis, means and standard errors of the mean estimate, are compared to previous analyses in Tables 2 and 3. For fixed values of channel radii our results for the other R-matrix parameters are somewhat close to the ones from Barker (2007). When fitted altogether, the strong correlation between partial widths and the channel radii leads to multi-modal posteriors and rather different estimated values of channel radii and partial widths. On the other

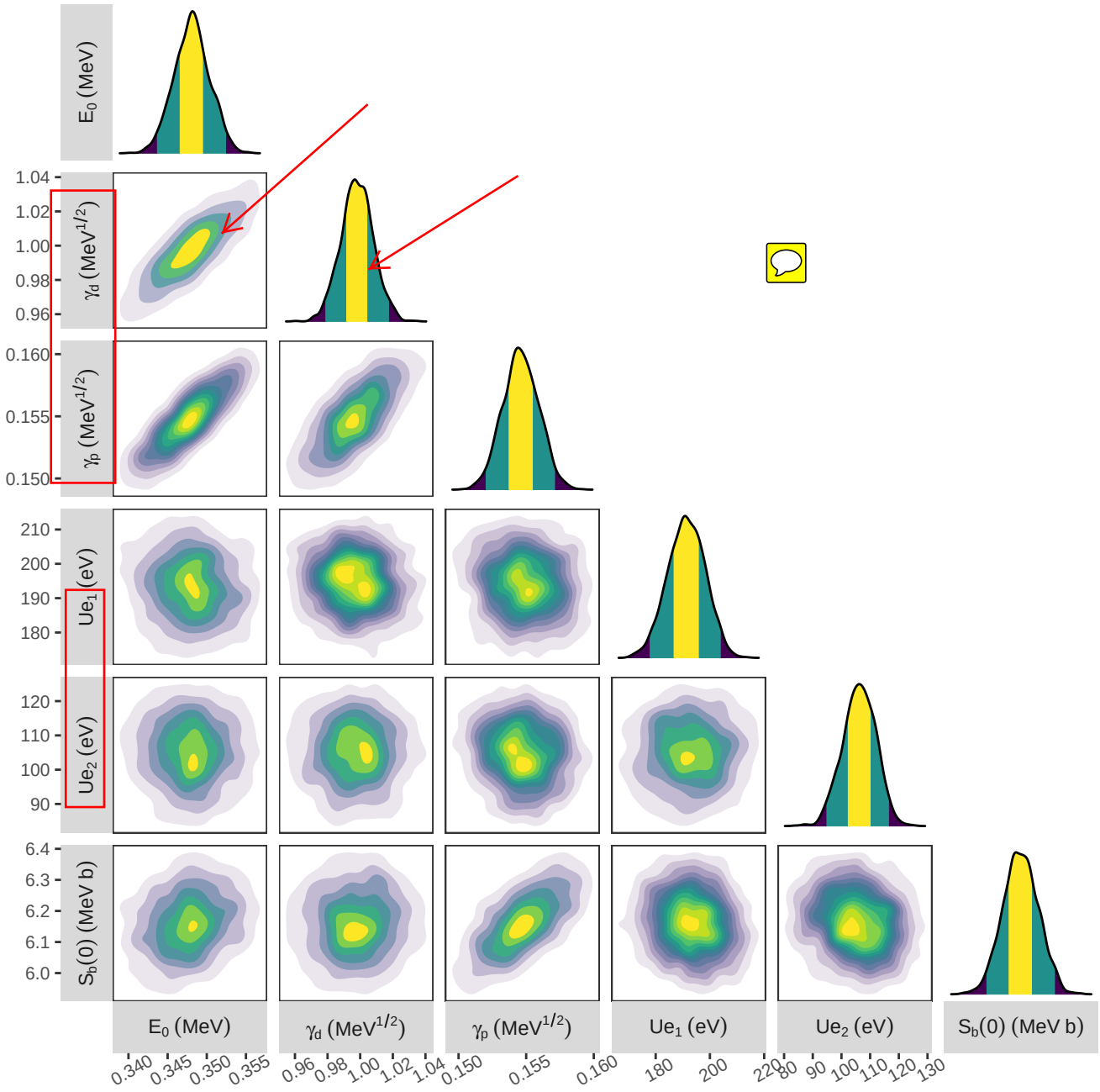

Figure 6. One- and two-dimensional marginalized posterior densities for the R-matrix parameters (E_0, γ_d, γ_p, U_e, and $S_b(0)$); see Section 2. The results were obtained for "~~case~~ I" (see Section 3.3.4). The contours in the panels for the two-dimensional densities represent 68% and 96% credible intervals.

hand, E_r show resilience against different prior choices and channel radii assumptions.

Table 3 highlights the summary information of the electron screening potentials for d(^{3}He,p)^{4}He and ^{3}He(d,p)^{4}He reactions. Our estimates $U_e = 105 \pm 10$ eV for d(^{3}He,p)^{4}He , and $U_e = 193 \pm 10$ eV for the ^{3}He(d,p)^{4}He . The values for ^{3}He(d,p)^{4}He are consistent with previous estimates from Barker (2007), and Descouvemont et al. (2004) within the uncertainties, but slightly lower than Aliotta et al. (2001), unlike the d(^{3}He,p)^{4}He , which shows a fair agreement with Aliotta et al. (2001), but is lower than Descouvemont et al. (2004). The S-factor at zero energy are overall consistent with previous estimates, although lower than Aliotta et al. (2001). We shall note that the current and previous estimated values are still larger than the so-called adiabatic limit – the difference in electron binding energies between the colliding atoms and the compound

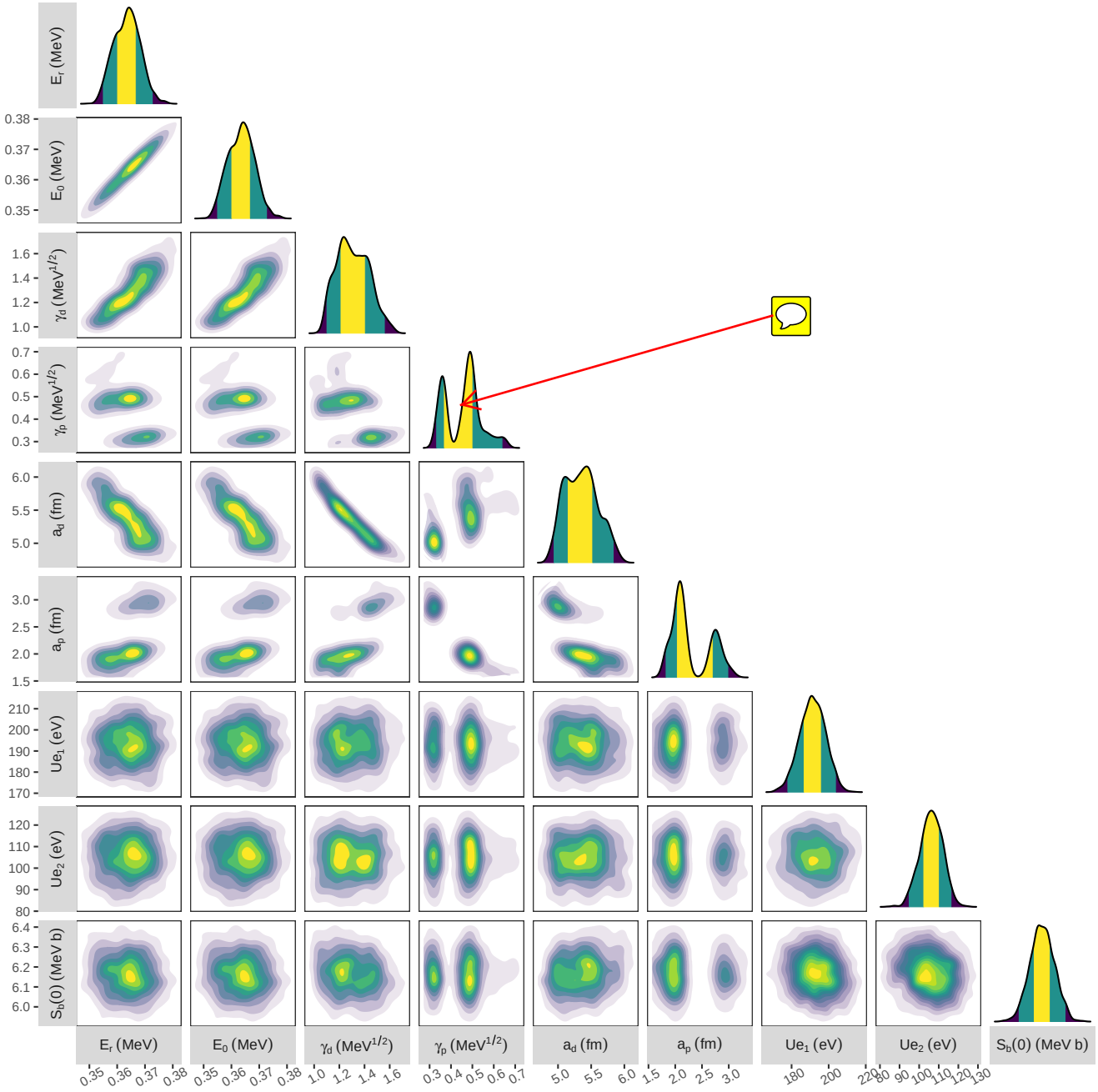

Figure 7. One- and two-dimensional marginalized posterior densities for the R-matrix parameters (E_0, E_r, γ_d^2, γ_p^2, a_d, and a_p); see Section 2. The results were obtained for "case I" (see Section 3.3.4). The contours in the panels for the two-dimensional densities represent 68% and 96% credible intervals.

atom – U_e = 65 eV for d(^{3}He,p)^{4}He, and U_e = 120 eV for ^{3}He(d,p)^{4}He (e.g., Aliotta et al. 2001), and such discrepancy are yet to be explained.

Finally, we show the probability distributions ~~for~~ the normalization factors ~~in Figure 3~~ for each data set. The vertical dashed red line represents zero systematic effects (i.e., a normalization factor of unity). ~~The normalization factors are mostly below 5% with 95% probability, indicating the absence of problematic experiments.~~ A summary statistics of the normalization factors are given in table 4

4.4. *Bayesian Reaction Rates*

The non-resonant thermonuclear reactions rates per particle pair is given by the Maxwellian-averaged rate times the Avogrado's number N_A:

Table 2. ~~Parameter values for R-matrix fit~~

	E_r	γ_p	γ_d	a_d	a_p
	MeV	$MeV^{1/2}$	$MeV^{1/2}$	fm	fm
Barker (2007)[b]	0.386	0.177	0.879	6	5
~~Case I~~	0.347 ± 0.004	0.155 ± 0.002	0.997 ± 0.020	6	5
~~Case II~~	0.363 ± 0.007	0.446 ± 0.107	1.307 ± 0.173	5.37 ± 0.32	2.27 ± 0.51

Table 3. Electron-screening ~~potential~~ and S-factors at zero-energy

	Ue_1	Ue_2	$S_b(0)$
	eV	eV	MeV b
NACRE II[a]	✗	✗	5.9 ± 0.5
Descouvemont et al. (2004)	201 ± 10	146 ± 5	5.9 ± 0.3
Barker (2007)[b]	194	✗	6.05
Aliotta et al. (2001)	219± 7	109± 9	6.7
~~Case I~~	193.28 ± 10.17	105.23 ± 10.19	6.160 ± 0.106
~~Case II~~	193.28 ± 10.17	105.23 ± 10.19	6.126 ± 0.10

[a] Xu et al. (2013).

Table 4. ~~Systematic uncertainties~~

~~Data~~	~~Normalization factor~~
Ali01a	0.993 ± 0.017
Ali01b	1.018 ± 0.017
Cos00	1.045± 0.023
Gei99	0.971± 0.017
Kra87	1.004 ± 0.010
Mol80	1.015 ± 0.01
Zhi77	0.973 ± 0.017

$$N_A \langle \sigma\nu \rangle = N_A \frac{(8/\pi)^{1/2}}{\mu_0^{1/2}(k_B T)^{3/2}} \int_0^\infty E\sigma(E) e^{-E/k_B T} dE$$

where $\sigma(E) \equiv S(E)e^{-2\pi\eta}/E$ is the reaction cross section at the center-of-mass incident energy $E = \mu v^2/2$ with v being the relative velocity. The term $\mu_0 = m_a m_b/(m_a + m_b)$ is the reduced mass with m_A and m_a standing for the masses of target (a) and projectile (b) nuclei, k_B is the Boltzmann constant, T the temperature, σ the cross section.

We estimate the reaction rates on a grid of temperatures from 1 MK to 10 GK, providing their mean values and uncertainties for both Cases I and II. The temperature grid, of 60 bins, is chosen to be consistent with previous works (Descouvemont et al. 2004), and to allow a seamless incorporation into the STARLIB library (Sallaska et al. 2013). Numerical reaction rate values are listed in Tables B, and 11. The recommended rates are computed as the 50th percentile of the probability density, while the rate factor uncertainty, f.u. $= e^{\sigma_L}$, with σ_L being the standard deviation of the lognormal posterior.

To illustrate the sensitivity of our results against the prior choice, figure 8 shows the ratio the nuclear rates between cases I and II. The agreement remains below 3% for the entire range of BBN interest with 99% probability.

5. SUMMARY AND CONCLUSIONS

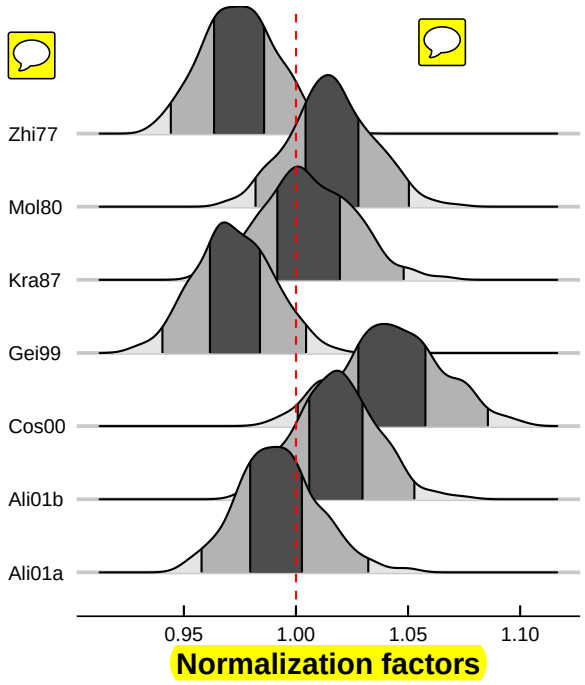

Posterior densities of the normalization factors, ξ_i, for each of the seven ~~datasets~~. **The shaded gray areas depicts 68% 95% and 99.5% credible intervals, respectively. For the data set labels, see Figure 5.**

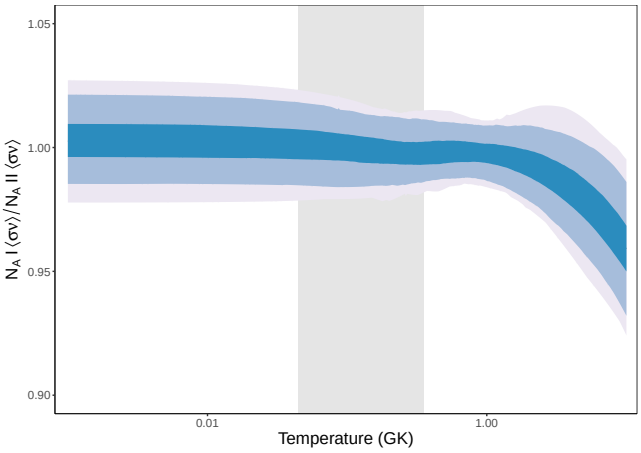

Figure 8. Ratios of the present reaction rates for Cases I and II. The shaded areas depicts 50%, 95%, and 99% credible intervals around the mean ratio.

The Big-Bang nucleosynthesis represents a milestone in the Universe evolution, being responsible for the production of the first light nuclides. Accurate measurements of the nuclear reaction rates occurring on this epoch are paramount to calibrate models chemical evolution. The connection between the theoretical cross-section, subsumed by the Astrophysical S-factor, and the laboratory da[illegible] not without issues, as the data is subject to several [illegible]rs of uncertainty, including intrinsic scatter, error-in-measurements and the effects of electron screening potential. Such stratified error-structure is not not amenable by standard approaches such as χ^2 minimization due to the normality deviation.

To overcame such limitation, we presented a framework to derive statistically sound reaction rates from d(^{3}He,p)^{4}He and ^{3}He(d,p)^{4}He data. The model was based on a hierarchical Bayesian framework. Our approach consistently accounts for stochastic uncertainties, errors-in-measurements, systematic effects, and the effects of the electron screening potential.

Here we presented the first statistically rigorous results for d+d reaction rate probability densities. These can be employed in future Monte Carlo studies of big bang nucleosynthesis.

We would like to thank xxx for their input and feedback. This work was supported in part by NASA under the Astrophysics Theory Program grant 14-ATP14-0007 and the U.S. DOE under Contract No. DE-FG02-97ER41041.

APPENDIX

A. NUCLEAR DATA FOR THE ^{3}HE(D,P)^{4}HE REACTION

A.1. *The ^{3}He(d,p)^{4}He data of Zhichang et al. (1977)*

The cross section data of Zhichang et al. (1977), as reported in EXFOR (2017), originate from a private communication by the authors and were adopted from Figure 2 of the original article. The derived experimental ~~S~~factors, together with their statistical ~~errors~~ ($\approx 0.6\%$) are listed in Table 5. The estimated systematic uncertainty is 3.4%, including the effects of target, solid angle, and beam intensity.

Table 5. The ^{3}He(d,p)^{4}He data of Zhichang et al. (1977).

$E_{c.m.} \pm \Delta E_{c.m.}$ (MeV)	$S \pm \Delta S_{\rm stat}$ [a] (MeVb)	$E_{c.m.} \pm \Delta E_{c.m.}$ (MeV)	$S \pm \Delta S_{\rm stat}$ [a] (MeVb)
0.1344±0.0048	10.074±0.060	0.2559±0.0042	15.950±0.095
0.1422±0.0047	12.080±0.072	0.2676±0.0042	14.505±0.087
0.1506±0.0047	12.544±0.075	0.2736±0.0041	14.194±0.085
0.1650±0.0046	12.375±0.074	0.2748±0.0041	14.231±0.085
0.1677±0.0045	14.590±0.087	0.2949±0.0041	12.757±0.076
0.1692±0.0045	15.314±0.092	0.3186±0.0041	10.505±0.063
0.1746±0.0045	15.760±0.095	0.3468±0.0040	9.188±0.055
0.1800±0.0044	15.987±0.096	0.3822±0.0040	6.773±0.040
0.1854±0.0044	17.415±0.104	0.4110±0.0039	5.863±0.035
0.1914±0.0044	18.116±0.109	0.4314±0.0038	5.071±0.030
0.1974±0.0044	17.763±0.107	0.4500±0.0037	4.695±0.028
0.2040±0.0044	17.728±0.106	0.4710±0.0037	4.411±0.026
0.2100±0.0044	17.825±0.107	0.5070±0.0036	3.761±0.022
0.2247±0.0043	17.502±0.105	0.5466±0.0035	3.002±0.018
0.2400±0.0043	16.640±0.099	0.5772±0.0034	2.999±0.018
0.2520±0.0042	15.987±0.096	0.6135±0.0033	2.364±0.014

[a] Systematic uncertainty: 3.4%.

A.2. *The ^{3}He(d,p)^{4}He and d(^{3}He,p)^{4}He data of Krauss et al. (1987)*

The Krauss et al. (1987) experiments took place at the ion accelerators in Münster and Bochum. Table 3 in Krauss et al. (1987) lists measured S-factors and statistical uncertainties. A normalization uncertainty of 6% originates from an absolute ^{3}He(d,p)^{4}He cross section measurement at a center-of-mass energy of 59.66 keV, to which a 5% uncertainty caused by variations in the alignment of beam and gas jet target profiles has to be added for the Münster data. Hence, we adopt a systematic uncertainty of 6.0% for the Bochum data and, following the authors, a value of 7.8% for the Münster data. Note that Krauss et al. (1987) do not report separately the results for ^{3}He(d,p)^{4}He and d(^{3}He,p)^{4}He. Since this distinction is important below a center-of-mass energy of 50 keV, we disregard all of their data points in this energy range. The data ~~that were~~ adopted for our analysis are listed in Table 6.

A.3. *The d(^{3}He,p)^{4}He data of Möller & Besenbacher (1980)*

In this experiment, the d(^{3}He,p)^{4}He differential cross section was measured at two angles~~,~~ relative to the d(d,p)^{3}H cross section. The total cross section was calculated using the angular distributions from (Yarnell et al. 1953). The statistical error is less than 3%, except at the lowest energy (7%). The systematic error, which arises from the normalization, the d(d,p)^{3}H cross section, and the anisotropy coefficient, amounts to 3.9%. The EXFOR cross section data were presumably scanned from Fig. 3 of (Möller & Besenbacher 1980). Our adopted S-factors are listed in Table 7.

A.4. *The ^{3}He(d,p)^{4}He and d(^{3}He,p)^{4}He data of Geist et al. (1999)*

The cross section data are presented in Figure 5 of Geist et al. (1999) and are available in tabular form from EXFOR, as communicated by the authors. Three data sets exist, one for the ^{3}He(d,p)^{4}He reaction and two for the d(^{3}He,p)^{4}He reaction~~, depending on the detected particle~~. The data are listed in Table 8, with statistical uncertainties only. We do

Table 6. The ^{3}He(d,p)^{4}He and d(^{3}He,p)^{4}He data of Krauss et al. (1987)[a].

$E_{c.m.}$ (MeV)	$S \pm \Delta S_{\rm stat}$[b] (MeVb)	$E_{c.m.}$[d] (MeV)	$S \pm \Delta S_{\rm stat}$[b] (MeVb)
0.04970[c]	7.24±0.07	0.0830	9.1±0.4
0.05369[c]	7.67±0.08	0.1007	9.9±0.5
0.05900[d]	8.4±0.4	0.1184	11.5±0.6
0.05952[c]	7.96±0.08	0.1360	13.1±0.6
0.05966[c]	8.26±0.08	0.1537	16.0±0.8
0.0653[d]	8.6±0.5	0.1713	17.2±0.9

[a] We disregarded all data points below a center-of-mass energy of 50 keV (see text).

[b] For some data points without reported statistical uncertainty, we assumed a value of 1%.

[c] Bochum data; systematic uncertainty: 6.0%.

[d] Münster data; systematic uncertainty: 7.8%.

not distinguish between the ^{3}He(d,p)^{4}He and d(^{3}He,p)^{4}He reactions because all data points were measured at center-of-mass energies above 50 keV ~~and, therefore,~~ electron screening effects can be disregarded. A systematic uncertainty of 4.3% is obtained by adding quadratically the contributions from the d(d,p)^{3}H monitor cross section scale and fitting procedure (1.3% and 3%, respectively), the incident beam energy and energy loss (2%), and the beam integration (2%).

A.5. *The d(^{3}He,p)^{4}He data of Costantini et al. (2000)*

We adopted the d(^{3}He,p)^{4}He results of Table 1 in Costantini et al. (2000), which lists the effective energy, ~~Sfactor~~, statistical uncertainty, and systematic uncertainty. The latter ranges from 8% at the lowest energy (4.22 keV) to 3.0% at the highest energy (13.83 keV). In our analysis, we assume an average systematic uncertainty of 5.5%. Table 9 lists the S-factors adopted in the present work.

A.6. *The ^{3}He(d,p)^{4}He and d(^{3}He,p)^{4}He data of Aliotta et al. (2001)*

The S-factor data for the ^{3}He(d,p)^{4}He and d(^{3}He,p)^{4}He ~~reaction~~ are taken from Tables 1 and 2, respectively, in Aliotta et al. (2001). The quoted uncertainties include only statistical (2.6%) effects. The systematic uncertainty arises from the target pressure, calorimeter, and detection efficiency, and amounts to 3.0%. The S-factor data adopted in the present work are listed in Table 10.

A.7. *Other data*

The following data sets were excluded from our analysis. Bonner et al. (1952) only present differential cross sections measured at zero degrees. The cross section data of Jarvis & Roaf (1953), obtained using photographic plates, are presented in their Table 1 for three bombarding energies. However, the origin of their quoted errors (6% − 14%) is not clear. Yarnell et al. (1953) report the differential cross section at 86° (see their Figure 6), but the bombarding energy uncertainty is large (3% − 14%) and the different contributions to the total cross section uncertainty cannot be estimated ~~separately~~ from the information provided. The latter argument also ~~hold~~ for the data of Freier & Holmgren (1954) (see their Figure 1). Arnold et al. (1954) provide cross ~~section~~ between 36 keV and 93 keV bombarding deuteron energy (see their Table 3), including a detailed error analysis. However it was suggested by Coc et al. (2015) that an unaccounted systematic error affected the d(d,n)^{3}He cross section measured in the same experiment. For the data of Kunz (1955), we could not estimate separately the statistical and systematic uncertainty contributions. We

Table 7. The d(^{3}He,p)^{4}He data of Möller & Besenbacher (1980).

$E_{c.m.}$ (MeV)	S (MeVb)	$\Delta S_{\rm stat}$ (MeVb)	$\Delta S_{\rm sys}$ (MeVb)
0.0856	7.17	0.50	0.28
0.1460	14.18	0.42	0.55
0.1736	16.68	0.50	0.65
0.2056	18.58	0.56	0.72
0.2196	17.24	0.52	0.67
0.2336	17.65	0.53	0.69
0.2668	14.77	0.44	0.58
0.2964	13.22	0.40	0.52
0.3088	11.22	0.34	0.44
0.3280	10.16	0.30	0.40
0.3856	7.34	0.22	0.29
0.4460	5.02	0.15	0.20
0.5064	3.87	0.12	0.15
0.5648	2.885	0.086	0.11
0.6256	2.337	0.070	0.090
0.6836	2.011	0.060	0.080
0.7504	1.681	0.050	0.070
0.8068	1.553	0.046	0.060

disregarded the data of La Cognata et al. (2005) because their indirect method does not provide absolute cross section values. They normalized their results to cross sections obtained in other experiments, mainly the data of Geist et al. (1999). See also the discussion in Barker (2007) regarding the absolute cross section normalization of La Cognata et al. (2005). We did not include the data of Engstler et al. (1988) and Prati et al. (1994) in our analysis because these results are biased by stopping-power problems. Finally, we also did not take into account the results of Barbui et al. (2013), who reported the plasma^{3}He(d,p)^{4}He S-factor using intense ultrafast laser pulses. The derivation of the S-factor versus center of mass energy from the measured Maxwellian-averaged cross section at different plasma temperatures is complicated and the systematic effects are not ~~apparent~~ to us.

B. REACTION RATES

REFERENCES

Aliotta, M., Raiola, F., Gyrky, G., et al. 2001, Nuclear Physics A, 690, 790 . http://www.sciencedirect.com/science/article/pii/S0375947401003669

Arnold, W. R., Phillips, J. A., Sawyer, G. A., Stovall, E. J., & Tuck, J. L. 1954, Phys. Rev., 93, 483. https://link.aps.org/doi/10.1103/PhysRev.93.483

Assenbaum, H. J., Langanke, K., & Rolfs, C. 1987, Zeitschrift für Physik A Atomic Nuclei, 327, 461. https://doi.org/10.1007/BF01289572

Bania, T. M., Rood, R. T., & Balser, D. S. 2002, Nature, 415, 54

Table 8. The ^{3}He(d,p)^{4}He and d(^{3}He,p)^{4}He data of Geist et al. (1999).

$E_{c.m.}$ (MeV)	$S \pm \Delta S_{\rm stat}$ [a] (MeVb)	$E_{c.m.}$ (MeV)	$S \pm \Delta S_{\rm stat}$ [a] (MeVb)
0.1527	15.89±0.11	0.3344	8.965±0.033
0.1645	16.76±0.21	0.3463	8.273±0.046
0.1762	17.07±0.14	0.3583	7.640±0.041
0.1880	17.36±0.20	0.3702	7.134±0.045
0.1899	17.418±0.067	0.3821	6.571±0.037
0.1999	17.40±0.15	0.3880	6.309±0.036
0.2017	17.562±0.094	0.1468	14.64±0.22
0.2117	17.38±0.23	0.1702	16.94±0.23
0.2236	16.36±0.21	0.1779	16.64±0.23
0.2255	16.635±0.070	0.2092	17.02±0.22
0.2374	15.86±0.12	0.2170	17.02±0.22
0.2493	15.08±0.12	0.2404	15.79±0.21
0.2612	14.12±0.10	0.2522	14.903±0.081
0.2732	13.300±0.045	0.2542	14.747±0.059
0.2746	13.399±0.052	0.2717	13.27±0.11
0.2851	12.181±0.077	0.2855	12.68±0.11
0.2866	12.464±0.083	0.3029	10.69±0.14
0.2971	11.520±0.079	0.3169	10.17±0.11
0.2985	11.428±0.064	0.3482	8.012±0.083
0.3089	10.474±0.090	0.3795	6.394±0.074
0.3105	10.598±0.055	0.4108	5.351±0.060
0.3224	9.6450±0.053		

[a] Systematic uncertainty: 4.3%.

Barbui, M., Bang, W., Bonasera, A., et al. 2013, Phys. Rev. Lett., 111, 082502. https://link.aps.org/doi/10.1103/PhysRevLett.111.082502

Barker, F. 2002, Nuclear Physics A, 707, 277 . http://www.sciencedirect.com/science/article/pii/S0375947402009211

Barker, F. C. 1997, Phys. Rev. C, 56, 2646. https://link.aps.org/doi/10.1103/PhysRevC.56.2646

—. 2007, Phys. Rev. C, 75, 027601. https://link.aps.org/doi/10.1103/PhysRevC.75.027601

Bonner, T. W., Conner, J. P., & Lillie, A. B. 1952, Phys. Rev., 88, 473. https://link.aps.org/doi/10.1103/PhysRev.88.473

Coc, A., Petitjean, P., Uzan, J.-P., et al. 2015, Phys. Rev. D, 92, 123526. https://link.aps.org/doi/10.1103/PhysRevD.92.123526

Coc, A., & Vangioni, E. 2010, Journal of Physics: Conference Series, 202, 012001. http://stacks.iop.org/1742-6596/202/i=1/a=012001

Cooke, R. J. 2015, The Astrophysical Journal Letters, 812, L12. http://stacks.iop.org/2041-8205/812/i=1/a=L12

Costantini, H., Formicola, A., Junker, M., et al. 2000, Physics Letters B, 482, 43 . http://www.sciencedirect.com/science/article/pii/S037026930000513X

Table 9. The d(^{3}He,p)^{4}He data of Costantini et al. (2000).

$E_{c.m.}$ (MeV)	$S \pm \Delta S_{\rm stat}$ [a] (MeVb)	$E_{c.m.}$ (MeV)	$S \pm \Delta S_{\rm stat}$ [a] (MeVb)
0.00422	9.7±1.7	0.00834	7.51±0.22
0.00459	9.00±0.67	0.00851	7.38±0.22
0.00471	8.09±0.62	0.00860	7.65±0.23
0.00500	8.95±0.70	0.00871	7.82±0.28
0.00509	9.8±1.0	0.00898	7.36±0.19
0.00537	8.86±0.48	0.00908	7.66±0.17
0.00544	8.01±0.39	0.00914	7.60±0.24
0.00551	9.68±0.70	0.00929	7.54±0.23
0.00554	8.87±0.55	0.00938	7.47±0.14
0.00577	8.99±0.31	0.00948	7.59±0.13
0.00583	8.93±0.36	0.00978	7.32±0.22
0.00590	8.74±0.25	0.00987	7.52±0.19
0.00593	8.31±0.55	0.00991	7.24±0.18
0.00623	8.15±0.29	0.01007	7.39±0.19
0.00631	8.10±0.23	0.01018	7.35±0.14
0.00652	8.26±0.48	0.01029	7.44±0.17
0.00657	8.03±0.26	0.01087	7.38±0.16
0.00672	8.32±0.16	0.01096	7.35±0.13
0.00700	7.90±0.27	0.01105	7.41±0.17
0.00707	8.32±0.28	0.01165	7.24±0.14
0.00734	7.70±0.16	0.01178	7.21±0.12
0.00740	7.69±0.15	0.01185	7.35±0.11
0.00746	7.90±0.18	0.01241	7.58±0.14
0.00752	7.83±0.26	0.01255	7.31±0.13
0.00812	7.31±0.11	0.01265	7.31±0.14
0.00819	7.31±0.25	0.01307	7.36±0.13
0.00822	7.43±0.24	0.01383	7.23±0.13
0.00829	7.85±0.24		

[a] Average systematic uncertainty: 5.5%.

Cyburt, R. H., Fields, B. D., Olive, K. A., & Yeh, T.-H. 2016, Reviews of Modern Physics, 88, 015004

Cyburt, R. H., Fields, B. D., Olive, K. A., & Yeh, T.-H. 2016, Rev. Mod. Phys., 88, 015004. https://link.aps.org/doi/10.1103/RevModPhys.88.015004

de Souza, R. S., Hilbe, J. M., Buelens, B., et al. 2015, MNRAS, 453, 1928

de Souza, R. S., Dantas, M. L. L., Krone-Martins, A., et al. 2016, MNRAS, 461, 2115

Descouvemont, P., Adahchour, A., Angulo, C., Coc, A., & Vangioni-Flam, E. 2004, Atomic Data and Nuclear Data Tables, 88, 203

Descouvemont, P., & Baye, D. 2010, Reports on Progress in Physics, 73, 036301

Table 10. The ^{3}He(d,p)^{4}He and d(^{3}He,p)^{4}He data of Aliotta et al. (2001)[a].

$E_{c.m.}$ (MeV)	$S \pm \Delta S_{\rm stat}$[c] (MeVb)	$E_{c.m.}$ (MeV)	$S \pm \Delta S_{\rm stat}$[c] (MeVb)
0.00501	10.8±1.5	0.02508	7.18±0.20
0.00550	10.31±0.81	0.02592[b]	7.17±0.19
0.00601	9.41±0.48	0.02662	6.93±0.18
0.00602	10.37±0.35	0.02788[b]	7.01±0.19
0.00645	9.36±0.35	0.02873	7.22±0.20
0.00690	8.82±0.31	0.02988[b]	7.19±0.19
0.00751	9.12±0.29	0.02991	6.87±0.18
0.00780	8.66±0.28	0.03110	7.24±0.20
0.00818	8.31±0.24	0.03190[b]	7.17±0.19
0.00896	7.85±0.26	0.03289	7.04±0.20
0.00902	7.88±0.22	0.03349	7.33±0.20
0.00966	7.68±0.22	0.03389[b]	7.43±0.20
0.01072	7.48±0.20	0.03586	7.22±0.18
0.01144	7.29±0.20	0.03589[b]	7.39±0.19
0.01195[b]	7.19±0.35	0.03589[b]	7.58±0.20
0.01199	7.35±0.20	0.03788[b]	7.63±0.20
0.01318	7.28±0.20	0.03858	7.33±0.18
0.01395[b]	6.95±0.23	0.03987[b]	7.65±0.20
0.01439	7.04±0.20	0.04067	7.44±0.22
0.01499	7.07±0.20	0.04187	7.29±0.20
0.01595[b]	6.87±0.18	0.04306	7.48±0.22
0.01675	7.16±0.20	0.04485	7.40±0.20
0.01794[b]	6.91±0.19	0.04544	7.70±0.22
0.01799	7.02±0.20	0.04786	7.63±0.20
0.01914	7.20±0.20	0.05021	7.66±0.22
0.01993[b]	6.75±0.18	0.05083	7.70±0.20
0.02094	6.81±0.18	0.05265	7.70±0.22
0.02155	7.09±0.20	0.05382	7.77±0.22
0.02192[b]	6.96±0.19	0.05504	7.77±0.22
0.02271	7.13±0.20	0.05681	7.88±0.20
0.02392[b]	6.92±0.19	0.05741	7.94±0.22
0.02393	6.91±0.18	0.05980	8.12±0.22

[a] S-factors obtained from ^{3}He(d,p)^{4}He measurement, unless noted otherwise.

[b] S-factors obtained from d(^{3}He,p)^{4}He measurement.

[c] Systematic uncertainty: 3.0%.

.

Table 11. Case I: Recommended reaction rates.[a]

T (GK)	Rate	Low Rate[b]	High Rate[b]	f.u.	T (GK)	Rate	Low Rate[b]	High Rate[b]	f.u.
0.001	3.6015E-19	3.6698E-19	3.7307E-19	1.019	0.14	2.8718E+05	2.9214E+05	2.9685E+05	1.018
0.002	6.2037E-13	6.3216E-13	6.4264E-13	1.019	0.15	3.8441E+05	3.9101E+05	3.9747E+05	1.018
0.003	6.4102E-10	6.5324E-10	6.6408E-10	1.019	0.16	5.0235E+05	5.1092E+05	5.1946E+05	1.018
0.004	5.0455E-08	5.1415E-08	5.2270E-08	1.019	0.18	8.0886E+05	8.2236E+05	8.3594E+05	1.017
0.005	1.1181E-06	1.1392E-06	1.1582E-06	1.018	0.2	1.2221E+06	1.2424E+06	1.2629E+06	1.017
0.006	1.1825E-05	1.2048E-05	1.2250E-05	1.018	0.25	2.8097E+06	2.8564E+06	2.9023E+06	1.017
0.007	7.7515E-05	7.8974E-05	8.0296E-05	1.018	0.3	5.3030E+06	5.3905E+06	5.4735E+06	1.017
0.008	3.6473E-04	3.7163E-04	3.7781E-04	1.018	0.35	8.7431E+06	8.8902E+06	9.0296E+06	1.017
0.009	1.3480E-03	1.3734E-03	1.3962E-03	1.018	0.4	1.3082E+07	1.3305E+07	1.3521E+07	1.017
0.01	4.1501E-03	4.2280E-03	4.2978E-03	1.018	0.45	1.8203E+07	1.8521E+07	1.8809E+07	1.017
0.011	1.1079E-02	1.1287E-02	1.1473E-02	1.018	0.5	2.3946E+07	2.4375E+07	2.4752E+07	1.017
0.012	2.6396E-02	2.6891E-02	2.7334E-02	1.018	0.6	3.6655E+07	3.7322E+07	3.7911E+07	1.017
0.013	5.7322E-02	5.8395E-02	5.9357E-02	1.018	0.7	5.0018E+07	5.0955E+07	5.1777E+07	1.017
0.014	1.1529E-01	1.1744E-01	1.1938E-01	1.018	0.8	6.3172E+07	6.4346E+07	6.5427E+07	1.017
0.015	2.1741E-01	2.2145E-01	2.2510E-01	1.018	0.9	7.5587E+07	7.6998E+07	7.8304E+07	1.018
0.016	3.8814E-01	3.9530E-01	4.0185E-01	1.018	1	8.6945E+07	8.8579E+07	9.0069E+07	1.018
0.018	1.0809E+00	1.1008E+00	1.1191E+00	1.018	1.25	1.1022E+08	1.1228E+08	1.1416E+08	1.018
0.02	2.6075E+00	2.6559E+00	2.7000E+00	1.018	1.5	1.2656E+08	1.2893E+08	1.3116E+08	1.018
0.025	1.5167E+01	1.5446E+01	1.5702E+01	1.018	1.75	1.3741E+08	1.4003E+08	1.4249E+08	1.018
0.03	5.7874E+01	5.8926E+01	5.9902E+01	1.018	2	1.4420E+08	1.4690E+08	1.4958E+08	1.018
0.04	4.0496E+02	4.1220E+02	4.1901E+02	1.018	2.5	1.4968E+08	1.5256E+08	1.5527E+08	1.018
0.05	1.6089E+03	1.6377E+03	1.6647E+03	1.018	3	1.4899E+08	1.5187E+08	1.5461E+08	1.018
0.06	4.6016E+03	4.6832E+03	4.7604E+03	1.018	3.5	1.4527E+08	1.4808E+08	1.5080E+08	1.018
0.07	1.0647E+04	1.0835E+04	1.1013E+04	1.018	4	1.4014E+08	1.4283E+08	1.4546E+08	1.018
0.08	2.1282E+04	2.1655E+04	2.2014E+04	1.018	5	1.2863E+08	1.3114E+08	1.3360E+08	1.019
0.09	3.8244E+04	3.8912E+04	3.9565E+04	1.018	6	1.1753E+08	1.1983E+08	1.2205E+08	1.019
0.1	6.3426E+04	6.4522E+04	6.5610E+04	1.018	7	1.0755E+08	1.0965E+08	1.1171E+08	1.019
0.11	9.8816E+04	1.0054E+05	1.0221E+05	1.018	8	9.8767E+07	1.0074E+08	1.0264E+08	1.019
0.12	1.4651E+05	1.4904E+05	1.5151E+05	1.018	9	9.1126E+07	9.2951E+07	9.4686E+07	1.019
0.13	2.0859E+05	2.1219E+05	2.1566E+05	1.018	10	8.4445E+07	8.6148E+07	8.7771E+07	1.02

[a] In units of $cm^3\ mol^1\ s^1$. The values correspond to the median rate, i.e., the 50th percentile of the rate probability density. The rate factor uncertainty, f.u., corresponding to a coverage probability of 68%, is calculated from f.u. $= e^{\sigma}$, where σ denotes the spread parameter of the lognormal approximation to the rate probability density.

[b] Low Rate = 16th, and High Rate = 84th percentiles respectively.

Table 12. Case II: Recommended reaction rates.

T (GK)	Rate	Low Rate[b]	High Rate[b]	f.u.	T (GK)	Rate	Low Rate[b]	High Rate[b]	f.u.
0.001	3.5985E-19	3.6620E-19	3.7277E-19	1.018	0.14	2.8776E+05	2.9271E+05	2.9712E+05	1.017
0.002	6.1990E-13	6.3086E-13	6.4210E-13	1.018	0.15	3.8522E+05	3.9193E+05	3.9777E+05	1.017
0.003	6.4057E-10	6.5193E-10	6.6348E-10	1.018	0.16	5.0354E+05	5.1230E+05	5.1986E+05	1.017
0.004	5.0419E-08	5.1313E-08	5.2219E-08	1.018	0.18	8.1090E+05	8.2508E+05	8.3708E+05	1.016
0.005	1.1172E-06	1.1371E-06	1.1571E-06	1.018	0.2	1.2261E+06	1.2465E+06	1.2651E+06	1.016
0.006	1.1816E-05	1.2026E-05	1.2238E-05	1.018	0.25	2.8213E+06	2.8657E+06	2.9080E+06	1.016
0.007	7.7454E-05	7.8840E-05	8.0221E-05	1.018	0.3	5.3183E+06	5.4073E+06	5.4880E+06	1.016
0.008	3.6449E-04	3.7101E-04	3.7749E-04	1.018	0.35	8.7698E+06	8.9165E+06	9.0501E+06	1.016
0.009	1.3471E-03	1.3712E-03	1.3952E-03	1.018	0.4	1.3126E+07	1.3341E+07	1.3542E+07	1.016
0.01	4.1473E-03	4.2213E-03	4.2949E-03	1.018	0.45	1.8261E+07	1.8567E+07	1.8837E+07	1.016
0.011	1.1072E-02	1.1270E-02	1.1466E-02	1.018	0.5	2.4013E+07	2.4429E+07	2.4780E+07	1.016
0.012	2.6379E-02	2.6850E-02	2.7316E-02	1.018	0.6	3.6752E+07	3.7396E+07	3.7939E+07	1.016
0.013	5.7286E-02	5.8307E-02	5.9322E-02	1.018	0.7	5.0151E+07	5.1039E+07	5.1791E+07	1.016
0.014	1.1522E-01	1.1727E-01	1.1931E-01	1.018	0.8	6.3360E+07	6.4464E+07	6.5466E+07	1.016
0.015	2.1728E-01	2.2114E-01	2.2499E-01	1.018	0.9	7.5825E+07	7.7154E+07	7.8368E+07	1.016
0.016	3.8787E-01	3.9477E-01	4.0166E-01	1.018	1	8.7273E+07	8.8764E+07	9.0197E+07	1.017
0.018	1.0802E+00	1.0994E+00	1.1186E+00	1.018	1.25	1.1070E+08	1.1263E+08	1.1451E+08	1.017
0.02	2.6064E+00	2.6525E+00	2.6988E+00	1.018	1.5	1.2731E+08	1.2953E+08	1.3169E+08	1.017
0.025	1.5160E+01	1.5428E+01	1.5695E+01	1.018	1.75	1.3843E+08	1.4083E+08	1.4320E+08	1.017
0.03	5.7847E+01	5.8862E+01	5.9885E+01	1.018	2	1.4548E+08	1.4796E+08	1.5050E+08	1.017
0.04	4.0486E+02	4.1187E+02	4.1899E+02	1.017	2.5	1.5137E+08	1.5403E+08	1.5673E+08	1.017
0.05	1.6094E+03	1.6367E+03	1.6649E+03	1.017	3	1.5109E+08	1.5376E+08	1.5645E+08	1.017
0.06	4.6036E+03	4.6819E+03	4.7614E+03	1.017	3.5	1.4773E+08	1.5030E+08	1.5293E+08	1.018
0.07	1.0654E+04	1.0836E+04	1.1015E+04	1.017	4	1.4284E+08	1.4538E+08	1.4794E+08	1.018
0.08	2.1301E+04	2.1664E+04	2.2019E+04	1.017	5	1.3175E+08	1.3413E+08	1.3649E+08	1.018
0.09	3.8287E+04	3.8939E+04	3.9567E+04	1.017	6	1.2087E+08	1.2308E+08	1.2530E+08	1.018
0.1	6.3503E+04	6.4591E+04	6.5625E+04	1.017	7	1.1104E+08	1.1309E+08	1.1516E+08	1.019
0.11	9.8952E+04	1.0067E+05	1.0225E+05	1.017	8	1.0237E+08	1.0431E+08	1.0623E+08	1.019
0.12	1.4670E+05	1.4926E+05	1.5156E+05	1.017	9	9.4791E+07	9.6630E+07	9.8420E+07	1.019
0.13	2.0892E+05	2.1255E+05	2.1579E+05	1.017	10	8.8173E+07	8.9895E+07	9.1588E+07	1.019

[a] In units of $cm^3\ mol^1\ s^1$. The values correspond to the median rate, i.e., the 50th percentile of the rate probability density. The rate factor uncertainty, f.u., corresponding to a coverage probability of 68%, is calculated from f.u. $= e^{\sigma}$, where σ denotes the spread parameter of the lognormal approximation to the rate probability density.

[b] Low Rate = 16th, and High Rate = 84th percentiles respectively.

Engstler, S., Krauss, A., Neldner, K., et al. 1988, Physics Letters B, 202, 179 . http://www.sciencedirect.com/science/article/pii/0370269388900032

EXFOR. 2017. http://www.nndc.bnl.gov/exfor/exfor.htm

Freier, G., & Holmgren, H. 1954, Physical Review, 93, 825

Gamow, G. 1948, Nature, 162, 680

Geist, W. H., Brune, C. R., Karwowski, H. J., et al. 1999, Phys. Rev. C, 60, 054003. https://link.aps.org/doi/10.1103/PhysRevC.60.054003

Gómez Iñesta, A., Iliadis, C., & Coc, A. 2017, The Astrophysical Journal, 849, 134. http://stacks.iop.org/0004-637X/849/i=2/a=134

Heinrich, J., & Lyons, L. 2007, Annual Review of Nuclear and Particle Science, 57, 145. https://doi.org/10.1146/annurev.nucl.57.090506.123052

Hilbe, J. M., de Souza, R. S., & Ishida, E. E. O. 2017, Bayesian Models for Astrophysical Data Using R, JAGS, Python, and Stan, doi:10.1017/CBO9781316459515

Iliadis, C., Anderson, K. S., Coc, A., Timmes, F. X., & Starrfield, S. 2016, The Astrophysical Journal, 831, 107. http://stacks.iop.org/0004-637X/831/i=1/a=107

Jarvis, R., & Roaf, D. 1953, Proceedings of the Royal Society of London A: Mathematical, Physical and Engineering Sciences, 218, 432. http://rspa.royalsocietypublishing.org/content/218/1134/432

Jaynes, E., & Bretthorst, G. 2003, Probability Theory: The Logic of Science (Cambridge University Press). https://books.google.com/books?id=tTN4HuUNXjgC

Krauss, A., Becker, H., Trautvetter, H., Rolfs, C., & Brand, K. 1987, Nuclear Physics A, 465, 150 . http://www.sciencedirect.com/science/article/pii/0375947487903022

Kunz, W. E. 1955, Physical Review, 97, 456

La Cognata, M., Spitaleri, C., Tumino, A., et al. 2005, Phys. Rev. C, 72, 065802. https://link.aps.org/doi/10.1103/PhysRevC.72.065802

Lane, A. M., & Thomas, R. G. 1958, Rev. Mod. Phys., 30, 257. https://link.aps.org/doi/10.1103/RevModPhys.30.257

Möller, W., & Besenbacher, F. 1980, Nuclear Instruments and Methods, 168, 111

Parent, E., & Rivot, E. 2012, Introduction to Hierarchical Bayesian Modeling for Ecological Data, Chapman & Hall/CRC Applied Environmental Statistics (Taylor & Francis). https://books.google.com/books?id=YYt-ZUTvbjUC

Peebles, P. J., & Ratra, B. 2003, Reviews of Modern Physics, 75, 559

Planck Collaboration, Adam, R., Ade, P. A. R., et al. 2016, A&A, 594, A1

Plummer, M. 2003, in Proceedings of the 3rd International Workshop on Distributed Statistical Computing

Prati, P., Arpesella, C., Bartolucci, F., et al. 1994, Zeitschrift für Physik A Hadrons and Nuclei, 350, 171. https://doi.org/10.1007/BF01290685

Riess, A. G., Filippenko, A. V., Challis, P., et al. 1998, AJ, 116, 1009

Sallaska, A. L., Iliadis, C., Champange, A. E., et al. 2013, ApJS, 207, 18

Savage, M. J., Scaldeferri, K. A., & Wise, M. B. 1999, Nuclear Physics A, 652, 273

Sbordone, L., Bonifacio, P., Caffau, E., et al. 2010, A&A, 522, A26. https://doi.org/10.1051/0004-6361/200913282

Spergel, D. N., Bean, R., Doré, O., et al. 2007, ApJS, 170, 377

Team, R. D. C. 2010, R: A language and environment for statistical computing, R Foundation for Statistical Computing, Vienna, Austria. http://www.r-project.org

Trotta, R. 2017, arXiv:1701.01467, arXiv:1701.01467

Xu, Y., Takahashi, K., Goriely, S., et al. 2013, Nuclear Physics A, 918, 61

Yarnell, J. L., Lovberg, R. H., & Stratton, W. R. 1953, Physical Review, 90, 292

Zhichang, L., Jingang, Y., & Xunliang, D. 1977, Atom. Ener. Sci. Tech., 129